Journal of Electromagnetic Waves and Applications, Vol. 7, No. 5, 631–649, 1993

Lossy Multistep Lamellar Gratings in Conical Diffraction Mountings: An Exact Eigenfunction Solution

S.-E. Sandström

The Institute of Theoretical Physics
Chalmers University of Technology
S-412 96, Göteborg, Sweden.

G. Tayeb, and R. Petit

Laboratoire d'Optique Electromagnétique
Centre de Saint-Jérôme
13397 Marseille Cedex 20, France

Abstract– The method of exact eigenfunctions has proven to be effective for the scalar grating problem. This makes it worthwhile to apply the method to the vectorial grating problem, also referred to as the problem of conical diffraction. The approach to exact eigenfunctions considered here relies on a refinement of approximate eigenvalues. For complicated gratings in particular, this technique reduces the numerical effort required to compute the vectorial eigenfunctions. Metallic and dielectric cavity-type structures as well as other structures with strong resonances are studied. Good convergence properties have been observed for a wide range of parameter values. The vectorial treatment of the case of general incidence provides new theoretical results for the color-separation problem.

INTRODUCTION

The technique to calculate the exact eigenfunctions for each grating layer has been employed in the past in the study of lamellar gratings [1–5]. This approach constitutes an alternative to methods based on Fourier expansion of the material parameters in the layers [6]. Another method, recently presented by Morf [7], employs an expansion of the field in each lamella in terms of Legendre polynomials. Results illustrating the properties of these three methods are detailed in an earlier report [8]. One finds that the performance of the method of exact eigenfunctions compairs favorably with that of the other two methods for the checkerboard grating studied in [7]. It has, moreover, proven to be superior to that of the Fourier technique [6] for all structures studied so far (particularly so when strong losses are involved) except for the limiting case where the period tends to zero. The so-called coupled-wave approach has been shown to have a convergence that is slower and less reliable than that of the method of exact eigenfunctions [9]. These results all pertain to the scalar case where the incident plane wave has a wave-vector that lies in the plane normal to the grating. The present paper treats the complete vector problem that arises at general incidence. Techniques for the related non-periodic problem with perfectly conducting boundaries are discussed in the literature [10].

The role of the periodicity, in this context, is that it allows the use of a discrete spectrum throughout. This is a welcome simplification when general material parameters are considered. The Fourier approach [6,8] has the drawback that it approximates discontinuous functions with series solutions in various ways. Any technique that does not treat the material as a continuum is more feasible in this respect and the method of exact eigenfunctions has, so far, proven to be the best. In this paper, we propose a concise formalism [11] for general lamellar structures. It is set up so as to avoid cumbersome component-manipulation and paves the way for a numerical implementation based on vector operations. The advantages of this approach are obvious when dealing with a plane-wave basis. Earlier work on this problem [12] is to a great extent formulated in terms of impedance concepts. A theoretical treatment of general incidence provides quantitative results for applications such as the design of gratings devised for the separation of colors in visible light [13]. This type of formalism is also amenable to certain types of frequency-selective surfaces and screens. This paper is divided into five sections. The first four sections describe the problem and the method and there then follows a discussion and a presentation of numerical results for a variety of grating structures.

I. PROBLEM DEFINITION

First, a few words on the problem setting. In order to study a lamellar geometry one would consider something like the grating profile shown in Fig. 1. This is a multistep lamellar grating (MSLG) with homogeneous lamellas. A layer q with thickness h^q is defined with respect to the origin by means of the distances $d_i^q (d_0^q = 0)$. A cross-section of the structure is presented in two dimensions because of the large number of parameters. Magnetic materials are not considered in the present paper ($\mu = \mu_0$ everywhere). With an incident plane wave (time convention: $\exp(-i\omega t)$) impinging in the direction specified by $-\hat{r}$ (cf. Fig. 2), the use of the standard spherical angles and the corresponding unit vectors comes naturally. The conical diffraction problem corresponds to $\phi \neq 0$; i.e. the incident wave-vector does not lie in the $x - z$ plane. The vector $\hat{p}$, defined by means of the angle ϕ_p, is either the polarization-vector of the incident E-field (E-field formulation) or the polarization-vector of the incident H-field (H-field formulation):

$$\begin{aligned} \overline{k} &= (k_x, k_y, k_z) = -k_0 \nu^0 (\sin\theta \cos\phi, \sin\theta \sin\phi, \cos\theta) = -k\hat{r} \\ \hat{p} &= \cos\phi_p \hat{\phi} + \sin\phi_p \hat{\theta} \end{aligned} \tag{1}$$

The method of exact eigenfunctions employs solutions to the field-equations that are specific to each layer. These solutions are referred to as vectorial eigenfunctions and linear combinations of these eigenfunctions are used to represent the total field in each layer. In order to compute the exact eigenfunctions for a layer, we first determine the corresponding eigenvalues. This is not an altogether trivial task [2,5] and the next section has, therefore, been devoted to an application of the matrix techniques used in [6 and 7].

II. APPROXIMATE EIGENVALUES

When focusing our attention on the eigenvalues, there are some observations that can be made. The method of exact eigenfunctions involves certain functions (f_E and f_H , cf. Appendix A) that define the eigenvalues of the structure. The complexity of these functions, and that of their derivatives in particular, increases rapidly with the complexity of the grating layers. It is, for this reason, impractical to calculate the eigenvalues by means of this formulation alone when one studies complicated structures where the layers have many lamellas per period [2,5]. An alternative strategy which leads to a matrix eigenvalue problem is useful in order to obtain approximations to the exact eigenvalues. The objective is to obtain sufficiently accurate approximate eigenvalues efficiently. To this end, we have used the well-known matrix approach [6–8]. The TE-TM decomposition, for example, can be used to show that the exact eigenvalues corresponding to general incidence are related to those of the scalar case through a simple modification of the wavenumbers (cf. Appendix A). With this in mind, let us now outline how the matrix technique is applied.

One is first inclined to consider the Fourier approach [6] to the scalar eigenvalue problems for the TE- and TM-polarization, respectively:

$$\left(\frac{d^2}{dx^2} + k_0^2 \nu(x)^2\right) \varphi = \left(\rho + k_y^2\right) \varphi \tag{2}$$

$$\left(\frac{d}{dx}\frac{1}{\nu(x)^2}\frac{d}{dx} + k_0^2\right) \varphi = \frac{\rho + k_y^2}{\nu(x)^2} \varphi \tag{3}$$

After having expanded the material parameters ν^2 or $1/\nu^2$ and the pseudoperiodic function φ in a complex Fourier series [6], a simple transformation leads to an algebraic eigenvalue problem that provides an approximation for the eigenvalue ρ. This approach works well for the TE-case. For the TM-case, however, Gibbs phenomenon tends to affect the accuracy a great deal when the discontinuities in $1/\nu^2$ are large.

In order to circumvent this problem one could use the approach suggested by Morf [7, 8]. Morf expands the field in each lamella separately in terms of Legendre polynomials. By imposing the matching conditions at the interfaces between the lamellas, one obtains an eigenvalue problem that is free of the shortcomings of the Fourier-series approach. If a grating layer is highly asymmetric (cf. Fig. 1), and since the same number of basis functions is used for each lamella, it may prove favorable to divide the longest lamella into two so as to obtain a better distribution of the basis functions. This feature, and the advantages of a formalism that is applicable to an arbitrary number of lamellas, are the reasons for considering a geometry with three lamellas in this paper. The two complementary methods that are described here are both instrumental in obtaining good approximate eigenvalues for all reasonable complex ν because of their different convergence properties.

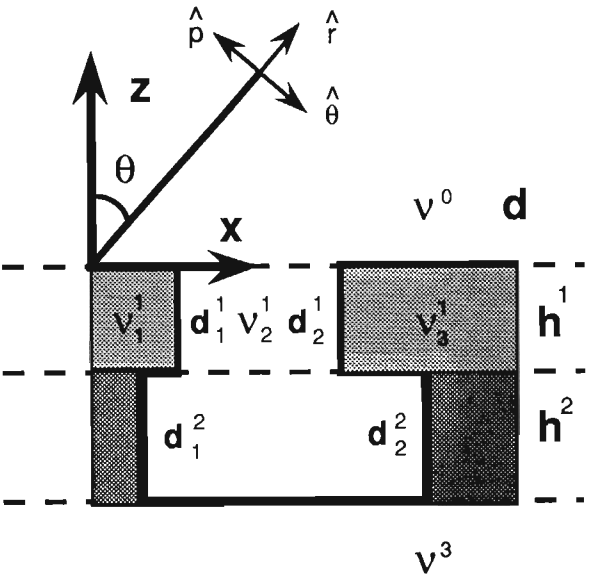

Figure 1. Cross-section of a grating with a period d. Superscripts and subscripts denote the layer and the lamella, respectively. The spherical unit-vectors $\hat{r}, \hat{\theta}$ that appear in this cut are shown for the case $\phi = 0°$ and the polarization vector $\hat{p}$ is shown for the case $\phi_p = -90°$.

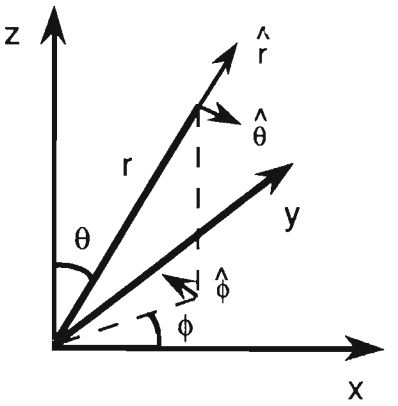

Figure 2. Spherical coordinates and unit vectors.

III. EXACT VECTORIAL EIGENFUNCTIONS

With material parameters that are piece-wise constant in a given layer, it is clear that some form of plane-wave solution is applicable for each lamella [8]. Equally apparent is the need for eigenfunctions that have a vector character (cf. [11] and Appendix A) and a y-dependence that corresponds to the incident field (cf. Eq. 1). Since the problem is separable in each lamella, and since the material parameters are constant in the vertical direction, the eigenfunction in a lamella denoted by the index i could involve the eigenvalue ρ in the following way:

$$\overline{\Psi}_i = \sum_{j=0}^{1} (\nabla_\times)^{1+j} \hat{p}_b \left\{ C_{0ji} e^{i\overline{\kappa}_{0i}\cdot(x-d_{i-1},y,z)} + C_{1ji} e^{i\overline{\kappa}_{1i}\cdot(x-d_i,y,z)} \right\} \qquad (4)$$

$$\kappa_{x0i} = \sqrt{k_0^2 \nu_i^2 - k_y^2 - \rho} \quad , \quad \kappa_{x1i} = -\kappa_{x0i} \quad , \quad \operatorname{Im} \kappa_{x0i} \geq 0$$

$$\kappa_y = k_y \quad , \quad \kappa_z = \sqrt{\rho} \quad , \quad \operatorname{Im} \kappa_z \geq 0$$

The idea is to express the eigenfunction in terms of vector-waves that are propagating or evanescent in either the positive or the negative x-direction. The exact eigenvalue ρ and the coefficients C_{0ji} and C_{1ji} are yet to be determined. Both the TE- and TM-eigenfunctions are of course present in disguised form in this formulation and materialize when the corresponding eigenvalues and coefficients are determined (cf. Appendix A). These eigenfunctions are transverse in the sense that the TE- and TM-modes have vanishing x-components for the E- and H-field, respectively. We allow ourselves to use the index j in the exponent for the vector differential-operator. This arrangement conforms to the formulation of the boundary conditions discussed below and it does also guarantee that the divergence of the eigenfunction equals zero [11]. For a plane-wave basis, the curl-operations correspond to vectorial multiplications. This simplifies the numerical implementation a great deal. The vector-basis approach used here is not restricted to electromagnetism [11] and treats E- and H-fields in essentially the same way. Allowing for a treatment of either the E- or the H-field for any polarization $\hat{p}$ implies a certain redundancy in the formalism; owing to the fact that the two incident field-types only differ by a rotation of the polarization, it would be sufficient to study E-fields, for example. This redundancy, in combination with a variation of $\hat{p}_b$, provides a test of the numerical implementation. The unit vector $\hat{p}_b$ is an arbitrary vector employed to construct the divergence-free vector basis [11] in Eq. (4). The only requirement that $\hat{p}_b$ has to fulfil is that it should not be parallel to $\hat{r}$ or to the wavevectors of any of the propagating orders (cf. section IV).

Having, thus, established the general form of the vectorial eigenfunction in an homogeneous lamella, it is straightforward to match the expressions for the various lamellas so as to cover the whole period. Depending on the field-type, the matching at an interface involves the continuity of either of the following entities:

$$\left.\begin{array}{l} \hat{x} \times (\nabla_\times)^j \overline{\Psi} \\ \hat{x} \times (\frac{\nabla_\times}{\nu^2})^j \overline{\Psi} \end{array}\right\} \quad j = 0, 1$$

If an E-field is considered, the first relation is applicable. The TE-eigenvalues then produce a transverse eigenfunction, whereas the TM-eigenvalues produce a non-transverse eigenfunction. Equation (5) and the pseudoperiodicity provide an homogeneous system of equations for the coefficients C_{0ji} and C_{1ji} and the determinantal condition for this system determines the exact eigenvalue ρ.

Since the eigenvalues can be extracted from the corresponding scalar problems (cf. Appendix A), this condition is more complicated than necessary, however. A more compact relation obtained by means of transmission matrices [4] is given in Appendix B. With the approximate eigenvalues discussed in section II as initial values, a root-finding procedure stands a good chance of locating the exact eigenvalues. A combination of the Muller and secant algorithms, reinforced with deflation, was used for this purpose. The method is reliable if all the initial values are sufficiently accurate; i.e. within a few percent of the exact eigenvalues. In order to obtain such an accuracy for all the desired approximate eigenvalues one has to treat a system that is larger than the size corresponding to the number of eigenvalues sought. This excess size is marginal for the TE-case but may at times be considerable for the TM-case. Some improvement can be obtained through the splitting of lamellas in asymmetric layers.

Finally, the eigenfunctions defined by the coefficients C_{0ji} and C_{1ji} follow from the homogeneous system corresponding to Eqs. (4) and (5). This approach eliminates a potential source of numerical error since the complete eigenfunctions are obtained from a linear system. Solutions to homogeneous systems of equations are often sensitive to small changes in the coefficients. As for the overall efficiency of this technique [2,5], one usually finds that the largest part of the total computer time spent on a problem is that devoted to the solution of the linear system discussed below. The time spent on other operations is almost negligible for structures with weak losses.

IV. THE SYSTEM OF EQUATIONS

With the exact eigenfunctions computed, the field in lamella i, in a layer with height h, can be expressed as a linear combination of a number of these eigenfunctions:

$$\begin{aligned} \overline{\Phi}_i \approx \sum_{n=0}^{2N} \sum_{p=0}^{1} \sum_{j=0}^{1} (\nabla\times)^{1+j} \hat{p}_b e^{i\kappa_y y} \\ \left[\left(C_{0ji0}^{np} e^{i\kappa_{x0i}^{np}(x-d_{i-1})} + C_{1ji0}^{np} e^{i\kappa_{x1i}^{np}(x-d_i)} \right) D_{0np}\, e^{i\kappa_z^{np} z} \right. \\ \left. + \left(C_{0ji1}^{np} e^{i\kappa_{x0i}^{np}(x-d_{i-1})} + C_{1ji1}^{np} e^{i\kappa_{x1i}^{np}(x-d_i)} \right) D_{1np}\, e^{-i\kappa_z^{np}(z-h)} \right] \end{aligned} \qquad (6)$$

$$\kappa_z^{np} = \sqrt{\rho^{np}} \quad , \quad \operatorname{Im} \kappa_z^{np} \geq 0$$

The indices n, p enumerate the eigenfunctions. p denotes the mode-type associated with a given eigenfunction; mode-types that in turn correspond to (2), (3), (B1) and (B2). With the branch-cut for κ_z chosen here, the field is expressed in terms of bounded exponentials. This promotes a good conditioning of the system of equations that emanates from the matching of solutions on the layer interfaces. For either field-type one is, once again, concerned with the continuity of the field and its curl:

$$\left.\begin{array}{l} \hat{z} \times (\nabla\times)^j \, \overline{\Phi} \\ \hat{z} \times \left(\dfrac{\nabla\times}{\nu^2}\right)^j \overline{\Phi} \end{array}\right\} \qquad j = 0, 1 \tag{7}$$

For the top and bottom layer, the ansatz is also matched against vectorial Rayleigh expansions propagating upwards and downwards, respectively. In the spirit of Eq. (6), these expansions are also set up as a divergence-free vector basis:

$$\overline{\Phi}_L \approx \sum_{n=-N}^{N} \sum_{j=0}^{1} (\nabla\times)^{1+j} \, \hat{p}_b \, e^{ik_x^n x} \, e^{ik_y y} \, e^{ik_{zL}^n z} E_{njL} \tag{8}$$

$$k_x^n = k_x + \frac{n2\pi}{d}$$

$$k_{zL}^n = (-)^L \sqrt{k_0^2 \nu_L^2 - k_y^2 - k_x^n} \quad , \quad \operatorname{Im} k_{z0}^n \geq 0 \quad , \quad L = 0, 1$$

The reflected, or transmitted (L=0 or 1; L denotes the superstrate and the substrate here), efficiencies are given by the expression:

$$e_{nL} \approx \sum_{j=0}^{1} \left| (\nabla\times)^{1+j} \, \hat{p}_b e^{ik_x^n x} \, e^{ik_y y} \, e^{ik_{zL}^n z} \right|^2 E_{njL} \, E_{njL}^* \frac{|k_{zL}^n| \, \nu_0^2}{k_{z0}^0 \, \nu_L^2} \tag{9}$$

The actual transformation to a linear system can be made by means of two scalar projections with respect to the Rayleigh basis. Here, all curl operations are replaced by the corresponding vector multiplications. Two tangential components [cf. (5)] provide relations that correspond to the two types of eigenfunctions. More precisely, one applies the following operator to the boundary condition that relates the fields to be matched:

$$\left\{ \begin{array}{l} \hat{x} \cdot \\ \hat{y} \cdot \end{array} \right\} \int_0^d e^{-ik_x^{n'} x} \, dx \tag{10}$$

The elementary integrals that arise from the projection are evaluated analytically. By carrying out this procedure for all the interfaces one obtains a linear system for the coefficients introduced in Eqs. (6) and (8). This exercise in index manipulation involves the incident source-field [cf. (1)] on the right hand side of the system and a suitably arranged set of projections on the left hand side. When the number of layers is large, a band structure appears in the coefficient matrix of the system. This property can be employed in the numerical treatment. If sufficiently accurate approximate eigenvalues are used, the final result has, so

far, been a well-conditioned system that can be solved accurately by means of standard techniques.

V. DISCUSSION AND NUMERICAL RESULTS

When applicable in the following examples, i.e. for lossless structures, the conservation of energy has been found to hold with a precision of five to eight significant figures as soon as a certain reasonable truncation of the system of equations is used. Such a threshold truncation is not noticeable for the scalar case [1,8]. For grating structures, one normally describes the diffraction by means of the efficiencies and the results are, therefore, given in terms of the computed efficiencies throughout the present paper. Commencing with a lossy structure, let us consider the results presented in Fig. 3. The zero-order reflected efficiency for an aluminum grating with a cavity-type profile is presented three-dimensionally as a function of the angles of incidence. An H-field with the polarization angle $\phi_p = 0°$ is taken to be the incident field. The wavelength is equal to the width of the cavity which gives rise to a number of resonances for small values of ϕ. These resonances are relatively weak, however, and since the "background" efficiency is rather large the phenomenon appears to be of limited interest. One may note that the resonant cavity is relatively open for this structure.

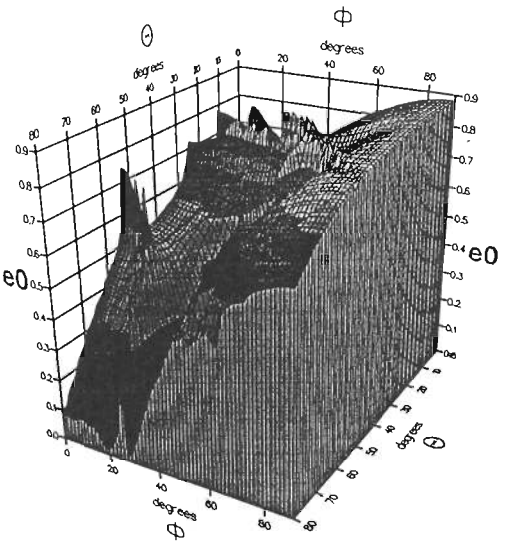

Figure 3. The graph gives a three-dimensional presentation of the reflected zero-order efficiency as a function of the angles of incidence for a geometry of the type shown in Fig. 1. An incident H-field with a polarization $\phi_p = 0°$ is considered. The parameters are: $\lambda/d = 0.6; d_1^1/d = 0.5, d_2^1/d = 0.65, \nu_1^1 = 1.5 + 8i, \nu_2^1 = 1, \nu_3^1 = 1.5 + 8i, h^1/d = 0.18; d_1^2/d = 0.2, d_2^2/d = 0.8, \nu_1^2 = 1.5 + 8i, \nu_2^2 = 1, \nu_3^2 = 1.5 + 8i, h^2/d = 20; \nu^0 = 1, \nu^3 = 1.5 + 8i$.

For the scalar case [8], the convergence rate of the solution was found to depend strongly on the polarization. Figure 4 presents the convergence rate of the grating efficiencies with respect to truncation for the conical problem discussed in conjunction with Fig. 3. It is apparent, from the results for the three polarizations considered here, that when the formalism does not separate into two scalar problems there can be a rather weak polarization-dependence. Unfortunately, but predictably, the convergence rate seems to resemble that of the TM-case rather than that of the TE-case [8]. The function $f(N)$ referred to in the graph corresponds to the maximum relative error in the calculated efficiencies. The orders in the Rayleigh expansions range from $-$N to N [cf. (6) and (8)] and the function f(N) essentially measures "the difference between two adjacent values of N" in terms of the number of significant figures.

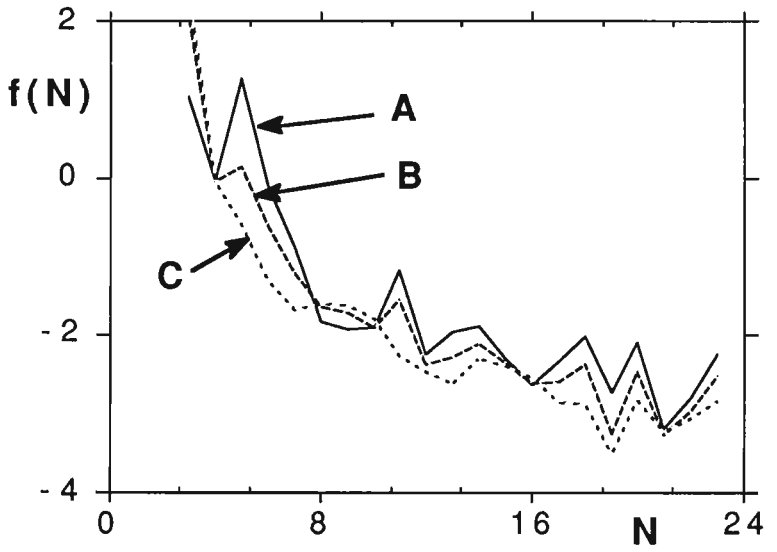

Figure 4. Convergence rate of the reflected efficiencies for the geometry considered in Fig. 3. The results are presented by means of the function $f(N) = \log_{10}(max_n(e_n^N - e_n^{N-1})/e_n^N)$ where the integer N defines the truncation. The incident H-field has the polarizations (A) $\phi_p = 0°$, (B) $\phi_p = 80°$, (C) $\phi_p = 90°$. The other parameters of incidence are: $\theta = 10°, \phi = 10°$.

Figure 5 shows the reflected zero-order efficiency for a dielectric cavity as a function of the angle of incidence. A rather sharp peak can be obtained after some adjustment of the parameters. A very narrow opening and the TM-polarization appears to be the recipe for this resonance. One might conjecture that adding another similar cavity under the first one would reinforce the resonance. So far,

no such effect has been observed, however. An example where the number of layers does affect the reflection properties considerably is the checkerboard grating [7]. This structure exhibits sharper and more symmetric resonances when the number of layers is increased from two to four. Four layers appears to be the optimum. Adding more layers has not been found to ameliorate the performance. Figure 6 presents the reflected zero-order efficiency for this grating as computed by means of the exact-eigenfunction technique. Its rapid convergence [8] makes these calculations feasible even when the number of layers is considerable. The preparation of Fig. 6 requires a numerical effort of the order of 1000 Gigaflops [14] if standard graphics and a large number of accurate data points are used. At normal incidence, a rotation in ϕ is equivalent to a change of polarization and the variation with respect to rotation is, therefore, rather slow.

Figure 7 illustrates how the resonance properties of a grating can be used to separate the colors in visible light [13]. When rotating the grating about the z-axis for a given incidence θ, a distinct change in the color of the reflected light can be observed. This effect is normally obtained by means of zero-order diffraction. By varying the polarization of the incident light, the relative intensity of the colors can be adjusted. A change in polarization has a minor effect on the position of the resonance in the $\lambda - \phi$ plane and could be used as a sort of fine-tuning of the radiation pattern. For this particular case, a polarization angle ϕ_p close to zero favors a strong resonance in the green, whereas an angle close to 90° yields a resonance that is the strongest in the red. At intermediate angles there is a widening, or even a splitting, of the peaks since resonances that seem to correspond to both the TE- and TM-polarizations are involved. As seen in the graph, the peaks are sufficiently sharp to cause problems in the graphical rendering. Figure 8 shows the same efficiency for a fixed rotation angle $\phi = 90°$; i.e. for the portion of the resonant spectrum that lies in the red. In this cut there are, first of all, two peaks and these peaks are in turn very acute. This behavior is typical and it is not surprising that the 3D representation fails to bring out all the details in data of this kind.

The results presented above illustrate how the method of exact eigenfunctions can be applied to rather complicated gratings. The limitation, as far as the number of layers goes, seems to be that imposed by the available memory-space since no insufficiency in the numerical stability has been observed. Certain parameter combinations might correspond to degenerate eigenfunctions but these combinations are very rare. The limit $d \to 0$ poses problems of a different type but for the scalar case the Fourier approach [6, 8] handles this limit without difficulty and it may, therefore, be possible to use Fourier techniques also for the vectorial case. Other than that, and disregarding the high-frequency limitations that are universal for modal methods, there are hardly any restrictions on the parameters. Therefore, and in conclusion, it is safe to say that the method of exact eigenfunctions is generally applicable also for the vectorial grating problem.

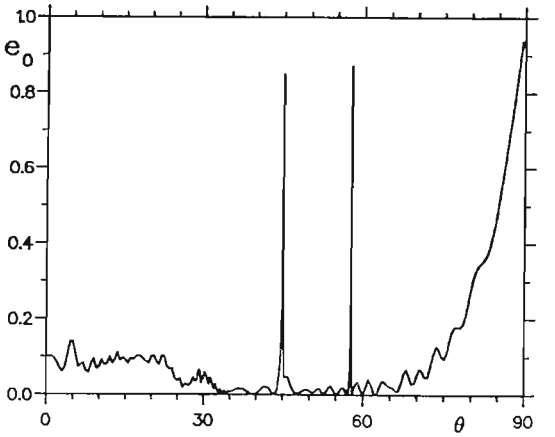

Figure 5. Reflected zero-order efficiency for a two-layer dielectric grating with a cavity as a function of the angle of incidence θ. An incident H-field ($\phi = 180°, \phi_p = 0°$) is studied. The parameters are: $\lambda/d = 0.6; d_1^1/d = 0.49, d_2^1/d = 0.51, \nu_1^1 = 1.5, \nu_2^1 = 1, \nu_3^1 = 1.5, h^1/d = 0.7; d_1^2/d = 0.2, d_2^2/d = 0.8, \nu_1^2 = 1.5, \nu_2^2 = 1, \nu_3^2 = 1.5, h^2/d = 15; \nu^0 = 1, \nu^3 = 1.5$.

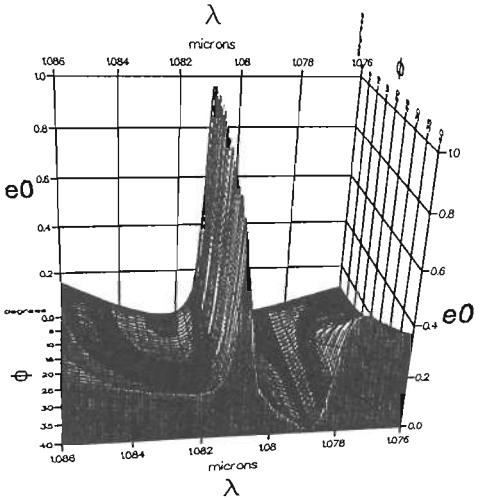

Figure 6. Reflected efficiency for a deep checkerboard grating illuminated by an H-field ($\phi_p = 0°$) at normal incidence. The results are computed as functions of the wavelength and the azimuth angle. The four-layer structure is made up of two identical double-layers stacked on top of each other. Parameters: $d = 1\mu; d_1^1/d = 0, d_2^1/d = 0.5, \nu_2^1 = 2.2, \nu_3^1 = 1.5, h^1/d = 3.2; d_1^2/d = 0, d_2^2/d = 0.5, \nu_2^2 = 1.5, \nu_3^2 = 2.2, h^2/d = 3.2; \nu^0 = 1, \nu^5 = 1$.

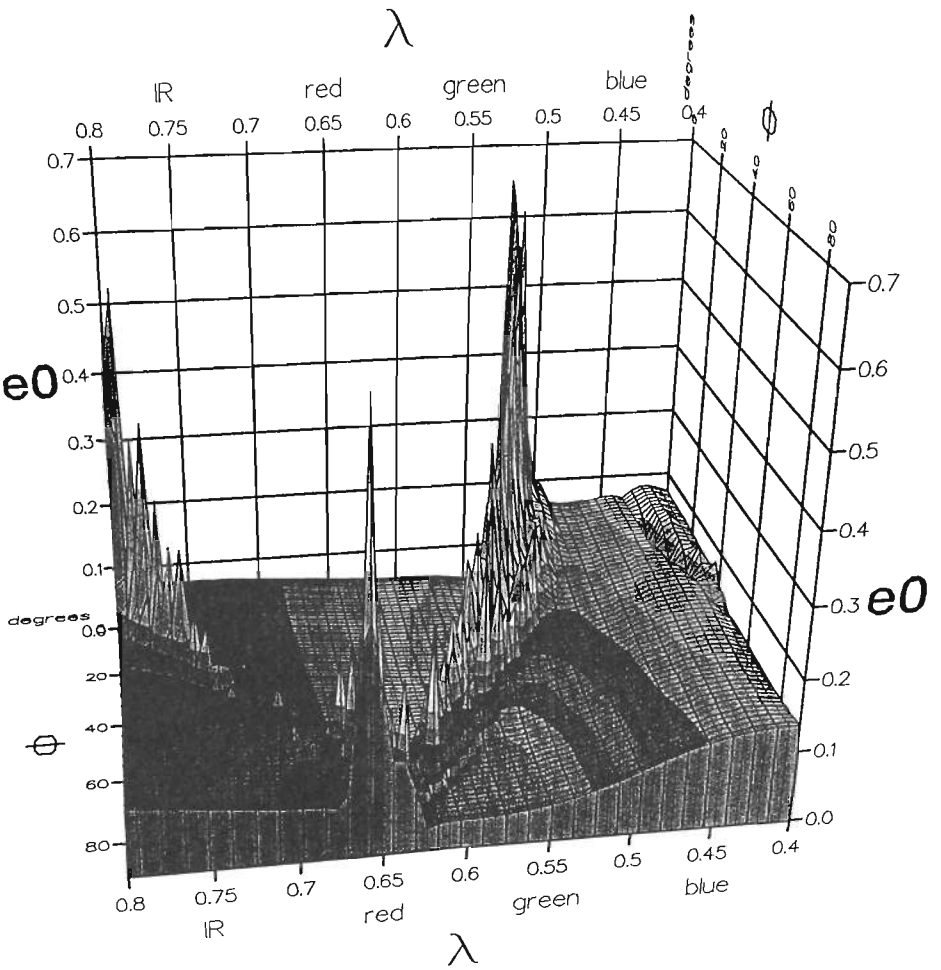

Figure 7. Reflected efficiency for order 0 for a one-layer color-separation structure as a function of the wavelength and the rotation angle: incident E-field $\phi_p = 0°, d = 0.44\mu, \theta = 22°; d_1^1/d = 0, d_2^1/d = 0.5, \nu_2^1 = 2, \nu_3^1 = 1.5, h^1/d = 0.38; \nu^0 = 1, \nu^2 = 1.5$.

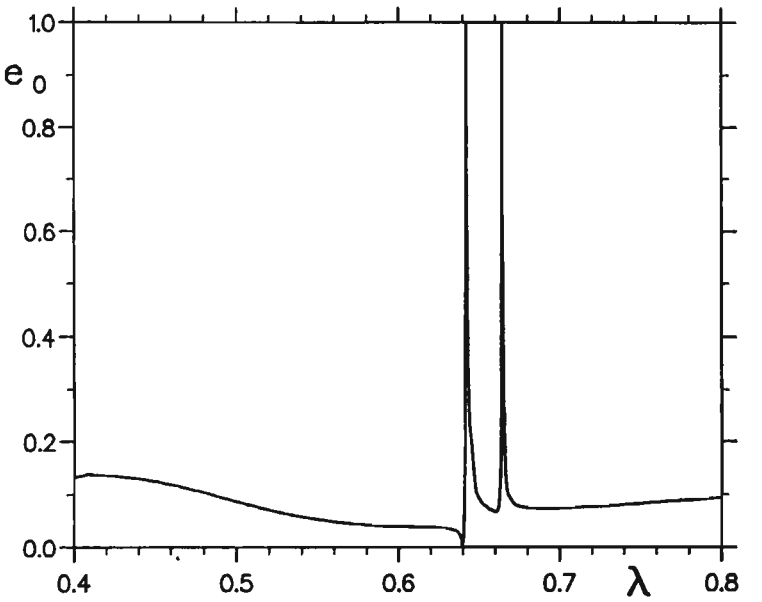

Figure 8. The reflected efficiency in Fig. 7 as a function of the wavelength only for the rotation angle $\phi = 90°$: incident E-field $\phi_p = 0°, d = 0.44\mu, \theta = 22°; d_1^1/d = 0, d_2^1/d = 0.5, \nu_2^1 = 2, \nu_3^1 = 1.5, h^1/d = 0.38; \nu^0 = 1, \nu^2 = 1.5$.

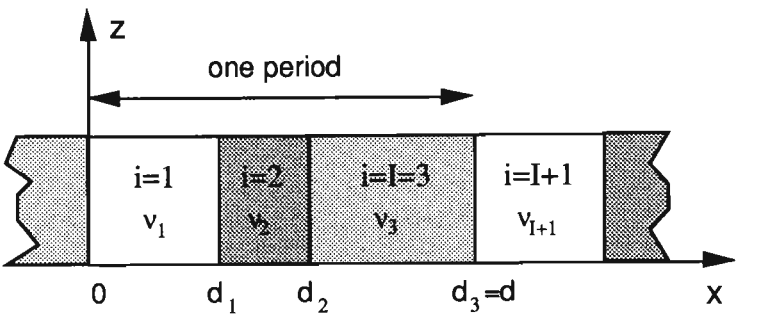

Figure 9. A grating layer with a period d. The notation used in this appendix differs slightly from that in the main paper for reasons of presentation.

APPENDIX A

In this appendix, our objective is to provide a more detailed presentation of the so-called eigenmodes inside a lamellar grating, for the case of conical diffraction (i.e. when the incident wave vector $\overline{k}$ is not perpendicular to the y axis). These vectorial eigenmodes can be expressed in terms of TE- and TM-modes: we speak of TE- (resp. TM-) modes when the electric (resp. magnetic) field has no component along the x axis. It will also appear that the eigenvalues associated with these TE- (resp. TM-) modes are linked in a very simple manner to those associated with the TE and TM cases of non-conical diffraction ($\overline{k} \cdot \hat{y} = 0.$). Moreover, the reader can find here some more details on a possible way to determine the vectorial eigenfunctions. Formally, the terms eigenmodes, eigenvalues and eigenfunctions are somewhat imprecise since the eigenvalue problem (operator, function spaces, etc.) is not clearly defined but we do not intend to elaborate on the mathematical aspects here.

In the layer depicted in Fig. 9, we study electromagnetic fields that: (a) satisfy Maxwell's equations and the continuity conditions on the interfaces $x = d_i$, $i = 1, 2, ..I$, (b) have the same y-dependency as the incident plane wave, (c) satisfy the pseudo-periodicity condition: any field component u must be such that $u(x+d, y, z) = u(x, y, z) \exp(ik_x d)$, where k_x is the x-component of the incident wave-vector.

Let us look for elementary solutions in each lamella. More precisely, in the lamella denoted by the integer i, it proves interesting to search the electric field as the sum of plane waves:

$$\overline{E}_i(x,y,z) = \overline{E}_i(\overline{r}) = \left\{ e_i^+ \, \overline{\kappa}_i^+ \times \hat{x} + h_i^+ \, \overline{\kappa}_i^+ \times \left(\overline{\kappa}_i^+ \times \hat{x} \right) \right\} e^{i\overline{\kappa}_i^+ \cdot \overline{r}} + \left\{ e_i^- \, \overline{\kappa}_i^- \times \hat{x} + h_i^- \, \overline{\kappa}_i^- \times \left(\overline{\kappa}_i^- \times \hat{x} \right) \right\} e^{i\overline{\kappa}_i^- \cdot \overline{r}} \quad (A1)$$

where

$$\overline{\kappa}_i^+ = (\kappa_{x,i}^+, \kappa_y, \kappa_z) \quad (A2)$$

$$\overline{\kappa}_i^- = (\kappa_{x,i}^-, \kappa_y, \kappa_z) \quad (A3)$$

$$\kappa_y = k_y = -k_0 \nu_0 \sin\theta \sin\phi \quad \text{(imposed by the incident plane wave)} \quad (A4)$$

$$\kappa_{x,i}^+ = -\kappa_{x,i}^- = \sqrt{k_i^2 - \kappa_y^2 - \kappa_z^2} \quad (A5)$$

(any branch-cut can be chosen for the complex square root)

$$k_i^2 = \overline{\kappa}_i^+ \cdot \overline{\kappa}_i^+ = \overline{\kappa}_i^- \cdot \overline{\kappa}_i^- = (k_0 \nu_i)^2 \quad (A6)$$

We have to find the eigenvalue $\rho = \kappa_z^2$ and, for each lamella, the coefficients $e_i^+, h_i^+, e_i^-, h_i^-$ that define the eigenfunction. Note that the expression $\left\{ e_i^+ \, \overline{\kappa}_i^+ \times \hat{x} + h_i^+ \, \overline{\kappa}_i^+ \times \left(\overline{\kappa}_i^+ \times \hat{x} \right) \right\} e^{i\overline{\kappa}_i^+ \cdot \overline{r}}$ can represent any plane wave with wave vector $\overline{\kappa}_i^+$ that verifies the divergence condition (i.e. the polarization is orthogonal to $\overline{\kappa}_i^+$). This decomposition is interesting in the sense that the first part

$e_i^+ \overline{\kappa}_i^+ \times \hat{x}$ is orthogonal to both the wave vector and the x axis, whereas the second part is orthogonal to the wave vector and to the first part. The other wave $\left\{e_i^- \overline{\kappa}_i^- \times \hat{x} \pm h_i^- \overline{\kappa}_i^- \times \left(\overline{\kappa}_i^- \times \hat{x}\right)\right\} e^{i\overline{\kappa}_i^- \cdot \overline{r}}$ differs in that the x-component of its wave vector has the opposite sign (A5).

In the ith homogeneous lamella, the magnetic field is derived from $\overline{E}_i$ by taking the curl:

$$\begin{aligned}\overline{H}_i(x,y,z) &= \frac{1}{\omega\mu_0}\left\{e_i^+ \overline{\kappa}_i^+ \times (\overline{\kappa}_i^+ \times \hat{x}) + h_i^+ \overline{\kappa}_i^+ \times \left(\overline{\kappa}_i^+ \times (\overline{\kappa}_i^+ \times \hat{x})\right)\right\} e^{i\overline{\kappa}_i^+ \cdot \overline{r}} \\ &\quad + \frac{1}{\omega\mu_0}\left\{e_i^- \overline{\kappa}_i^- \times (\overline{\kappa}_i^- \times \hat{x}) + h_i^- \overline{\kappa}_i^- \times \left(\overline{\kappa}_i^- \times (\overline{\kappa}_i^- \times \hat{x})\right)\right\} e^{i\overline{\kappa}_i^- \cdot \overline{r}} \\ &= \frac{1}{\omega\mu_0}\left\{e_i^+ \overline{\kappa}_i^+ \times (\overline{\kappa}_i^+ \times \hat{x}) - h_i^+ \kappa_i^2 \overline{\kappa}_i^+ \times \hat{x}\right\} e^{i\overline{\kappa}_i^+ \cdot \overline{r}} \\ &\quad + \frac{1}{\omega\mu_0}\left\{e_i^- \overline{\kappa}_i^- \times (\overline{\kappa}_i^- \times \hat{x}) - h_i^- \kappa_i^2 \overline{\kappa}_i^- \times \hat{x}\right\} e^{i\overline{\kappa}_i^- \cdot \overline{r}} \qquad (A7)\end{aligned}$$

It now appears that the coefficients e_i^+, e_i^-, (resp. h_i^+, h_i^-), correspond to the part of the field whose electric (resp. magnetic) field has no component along the x axis. Equation (A5) ensures that these fields satisfy Maxwell's equations in each homogeneous lamella.

In order to determine the entities $\kappa_z, e_i^+, h_i^+, e_i^-, h_i^-$, we must first enforce the continuity of the fields at $x = d_i$, when passing from lamella i to lamella $i+1$:

$$\hat{x} \times \overline{E}_i = \hat{x} \times \overline{E}_{i+1} \quad , \quad \hat{x} \times \overline{H}_i = \hat{x} \times \overline{H}_{i+1} \quad , \quad i = 1, 2, \ldots, I \quad (A8)$$

These four conditions can be written as,

$$\begin{pmatrix} e_{i+1}^+ \\ e_{i+1}^- \end{pmatrix} = \overline{\overline{M}}_{E,i} \begin{pmatrix} e_i^+ \\ e_i^- \end{pmatrix} \quad \text{and} \quad \begin{pmatrix} h_{i+1}^+ \\ h_{i+1}^- \end{pmatrix} = \overline{\overline{M}}_{H,i} \begin{pmatrix} h_i^+ \\ h_i^- \end{pmatrix} \qquad (A9)$$

where there is no coupling between the "e" and "h" coefficients. It is not necessary for our purpose to give the explicit form of the 2x2 matrices $\overline{\overline{M}}_{E,i}$ and $\overline{\overline{M}}_{H,i}$. This problem is nothing other than the problem of reflection and transmission of plane waves at an interface. For the ensuing treatment, it suffices to notice that these matrices involve the entities $\kappa_{x,i}^+, \kappa_{x,i+1}^+, \nu_i, \nu_{i+1}$ and d_i

The last step is to make use of the pseudo-periodicity condition. After some elementary calculations, this condition takes the form:

$$\begin{pmatrix} e_{I+1}^+ \\ e_{I+1}^- \end{pmatrix} = \overline{\overline{D}}_E \begin{pmatrix} e_1^+ \\ e_1^- \end{pmatrix} \quad \text{and} \quad \begin{pmatrix} h_{I+1}^+ \\ h_{I+1}^- \end{pmatrix} = \overline{\overline{D}}_H \begin{pmatrix} h_1^+ \\ h_1^- \end{pmatrix} \qquad (A10)$$

The diagonal 2x2 matrices $\overline{\overline{D}}_E$ and $\overline{\overline{D}}_H$ involve the entities $\kappa_{x,1}^+, k_x$ and the grating period d. From (A9) and (A10) we obtain:

$$\begin{pmatrix} e_{I+1}^+ \\ e_{I+1}^- \end{pmatrix} = \overline{\overline{D}}_E \begin{pmatrix} e_1^+ \\ e_1^- \end{pmatrix} = \overline{\overline{M}}_{E,I} \cdots \overline{\overline{M}}_{E,2} \overline{\overline{M}}_{E,1} \begin{pmatrix} e_1^+ \\ e_1^- \end{pmatrix} \qquad (A11)$$

$$\begin{pmatrix} h_{I+1}^+ \\ h_{I+1}^- \end{pmatrix} = \overline{\overline{D}}_H \begin{pmatrix} h_1^+ \\ h_1^- \end{pmatrix} = \overline{\overline{M}}_{H,I} \cdots \overline{\overline{M}}_{H,2} \overline{\overline{M}}_{H,1} \begin{pmatrix} h_1^+ \\ h_1^- \end{pmatrix} \qquad (A12)$$

and

$$\left(\overline{\overline{D}}_E - \overline{\overline{M}}_{E,I} \cdots \overline{\overline{M}}_{E,2}\,\overline{\overline{M}}_{E,1}\right)\begin{pmatrix} e_1^+ \\ e_1^- \end{pmatrix} = 0 \qquad (A13)$$

$$\left(\overline{\overline{D}}_H - \overline{\overline{M}}_{H,I} \cdots \overline{\overline{M}}_{H,2}\,\overline{\overline{M}}_{H,1}\right)\begin{pmatrix} h_1^+ \\ h_1^- \end{pmatrix} = 0 \qquad (A14)$$

In order for these two homogeneous systems to have non-trivial solutions, their determinants f_E and f_H must vanish (we recall below the parameters that are involved in these determinants):

$$f_E\left(\sqrt{k_i^2 - \kappa_y^2 - \rho},\, k_x,\, \nu_i,\, d_i,\, d\right) \stackrel{\text{def}}{=} \det(\overline{\overline{D}}_E - \overline{\overline{M}}_{E,I} \cdots \overline{\overline{M}}_{E,2}\,\overline{\overline{M}}_{E,1})$$
$$= 0 \qquad (A15)$$

$$f_H\left(\sqrt{k_i^2 - \kappa_y^2 - \rho},\, k_x,\, \nu_i,\, d_i,\, d\right) \stackrel{\text{def}}{=} \det(\overline{\overline{D}}_H - \overline{\overline{M}}_{H,I} \cdots \overline{\overline{M}}_{H,2}\,\overline{\overline{M}}_{H,1})$$
$$= 0 \qquad (A16)$$

In conclusion there exists TE and TM vectorial eigenmodes. For the TE modes, $h_i^+ = h_i^- = 0, \rho = \kappa_z^2$ is a root of (A15) and, as soon as ρ is known, the coefficients e_i^+ and e_i^- are given (within a multiplicative factor) by (A13) and (A9). For the TM modes, $e_i^+ = e_i^- = 0$, ρ is a root of (A16) and the coefficients h_i^+ and h_i^- are obtained analogously. N.B. We are well aware that we do not prove that the field can always be expressed as a linear combination of these TE and TM eigenmodes. For the present time, the completeness remains a conjecture based on reliable numerical results.

Finding ρ as a root of (A15) or (A16) is not a simple matter since ρ is generally complex. Fortunately, we can benefit by earlier work on non-conical diffraction (i.e. $k_y = 0$). For non-conical diffraction, we know that the problem splits into two scalar problems: the TE- and the TM-case with the electric and the magnetic fields, respectively, parallel to the y axis. Since the vector $\overline{\kappa}_i^+ \times \hat{x} = \overline{\kappa}_i^- \times \hat{x} = (0, \kappa_z, -\kappa_y)$, which was up to now perpendicular to $\hat{x}$, becomes parallel to $\hat{y}$ when $k_y = 0$, equations (A1) and (A7) show that the non-conical TE (resp. TM) case is obtained by simply replacing κ_y, h_i^+, h_i^- (resp. κ_y, e_i^+, e_i^-) by zero everywhere. Consequently, the eigenvalues $\tilde{\rho} = \tilde{\kappa}_z^2$ of the non-conical case are obtained by solving the equations deduced from (A15) and (A16) replacing $k_y = \kappa_y$ by zero:

$$f_E\left(\sqrt{k_i^2 - \tilde{\rho}},\, k_x,\, \nu_i,\, d_i,\, d\right) = 0 \qquad \text{for the non-conical TE case} \qquad (A17)$$

$$f_H\left(\sqrt{k_i^2 - \tilde{\rho}},\, k_x,\, \nu_i,\, d_i,\, d\right) = 0 \qquad \text{for the non-conical TM case} \qquad (A18)$$

Comparing (A15), (A16) and (A17), (A18), we infer that for conical diffraction the eigenvalues can be obtained from any computer program developed for non-conical diffraction by means of the following recipe: (a) find the eigenvalues $\tilde{\rho} = \tilde{\kappa}_z^2$ of the non-conical problem with the same opto-geometrical parameters and the

same pseudo-periodicity (i.e. the same k_x) as the conical problem in question, (b) obtain the eigenvalues of the conical problem from the relation $\rho = \tilde{\rho} - \kappa_z^2$.

A reader familiar with the study of lamellar gratings in classical mountings ($k_y = 0$) may recall that the solutions $\tilde{\rho}$ of (A17) are also eigenvalues of the operator $\mathcal{L}_E$ acting on pseudo-periodic scalar functions [4]:

$$\mathcal{L}_E = \frac{d^2}{dx^2} + k_0^2 \nu^2(x) \tag{A19}$$

Likewise, the solutions of (A18) are eigenvalues of an operator $\mathcal{L}_H$:

$$\mathcal{L}_H = \nu^2(x) \left[\frac{d}{dx} \left(\frac{1}{\nu^2(x)} \frac{d}{dx} \right) + k_0^2 \right] \tag{A20}$$

These operators play an important role in the search for approximate solutions to Eqs. (A17) and (A18).

APPENDIX B

For a slightly simplified case with $\kappa_1^q = \kappa_3^q = \kappa_2, \kappa_2^q = \kappa_1$ and $\nu_1^q = \nu_3^q = \nu_2, \nu_2^q = \nu_1$, the exact eigenvalues for the TM-case are zeros of the following function:

$$\begin{aligned} f(\rho) = &- \sin(\kappa_2 d_1) \left[\left\{ \frac{\kappa_1 (\nu_2)^2}{\kappa_2 (\nu_1)^2} + \frac{\kappa_2 (\nu_1)^2}{\kappa_1 (\nu_2)^2} \right\} A + 2B \right] \\ &+ \cos \kappa_2 d_1 \left[2D - \left\{ \frac{\kappa_1 (\nu_2)^2}{\kappa_2 (\nu_1)^2} + \frac{\kappa_2 (\nu_1)^2}{\kappa_1 (\nu_2)^2} \right\} C \right] - 2 \cos(k_x d) \end{aligned} \tag{B1}$$

The zeros for the TE-case are obtained by letting $\nu_1 = \nu_2 = 1$ in (B1) while leaving the following expressions unchanged:

$$\begin{aligned} A &= \cos \kappa_2 (d - d_2) \sin \kappa_1 (d_2 - d_1) \\ B &= \cos \kappa_1 (d_2 - d_1) \sin \kappa_2 (d - d_2) \\ C &= \sin \kappa_1 (d_2 - d_1) \sin \kappa_2 (d - d_2) \\ D &= \cos \kappa_1 (d_2 - d_1) \cos \kappa_2 (d - d_2) \\ \kappa_1 &= \sqrt{k_0^2 (\nu_1)^2 - k_y^2 - \rho} \\ \kappa_2 &= \sqrt{k_0^2 (\nu_2)^2 - k_y^2 - \rho} \end{aligned} \tag{B2}$$

Since the complexity of these expressions increases rapidly with the number of lamellas, it quickly becomes an arduous task to evaluate the derivatives [2,5].

ACKNOWLEDGMENTS

One of the authors (S.-E. S.) is supported financially by a French government D.R.E.D. post-doctoral bursary.

The Editor thanks S. L. Chuang, A. A. Maradudin, and M. Y. Zhou for reviewing the paper.

REFERENCES

1. Botten, L. C., M. S. Craig, R. C. Mc Phedran, J. L. Adams, and J. R. Andrewartha, "The dielectric lamellar diffraction grating," *Optica Acta,* Vol. 28, 413–428, 1981, *ibid.,* "The finitely conducting lamellar diffraction grating," 1087–1102.
2. Botten, L. C., M. S. Craig, and R. C. Mc Phedran, "Highly conducting lamellar diffraction gratings," *Optica Acta,* Vol. 28, 1103–1106, 1981.
3. Sheng, P., R. S. Stepleman, and P. N. Sanda, "Exact eigenfunctions for square-wave gratings: Application to diffraction and surface-plasmon calculations," *Phys. Rev.,* Vol. B 26, 2907–2916, 1982.
4. Suratteau, J. Y., M. Cadilhac, and R. Petit, "On the numerical study of deep dielectric lamellar gratings," *URSI Proceedings,* Santiago de Compostella, 179–182, 1983.
5. Tayeb, G., and R. Petit, "On the numerical study of deep conducting lamellar diffraction gratings," *Optica Acta,* Vol. 31, 1361–1365, 1984.
6. Knop, K., "Rigorous diffraction theory for transmission phase gratings with deep rectangular grooves," *J. Opt. Soc. Am.,* Vol. 68, 1206–1210, 1978.
7. Morf, R., "Diffraction theory - DOE efficiency," contribution to the Workshop on *Optical Information Technology* (WOIT), 1991.
8. Sandström, S.-E., G. Tayeb, and R. Petit, "Some comments on the use of exact eigenfunctions for lossy lamellar gratings," *LOE Internal Report,* Centre de Saint-Jérôme, 13397 Marseille Cedex 20, France, March 1992.
9. Li, L., and C. W. Haggans, "On the convergence of the coupled-wave approach for lamellar gratings," *OSA Conference Proceedings,* New Orleans, April 1992.
10. Kok, Y.-L., "Boundary-value solution to electromagnetic scattering by a rectangular groove in a ground plane," *J. Opt. Soc. Am.,* Vol. A 9, 302–311, 1992.
11. Morse, P. M., and H. Feshbach, *Methods of Theoretical Physics,* Part II, Chapter 13. McGraw-Hill, New York, 1953.
12. Peng, S. T., "Rigorous formulation of scattering and guidance by dielectric grating waveguides: general case of oblique incidence," *J. Opt. Soc. Am.,* Vol. A 6, 1869–1883, 1989.
13. Gale, M. T., K. Knop, and R. Morf, "Zero-order diffractive microstructures for security applications," *SPIE Proceedings Reprint,* 1210, 83–89, 1990.
14. Dongarra, J. J., "Performance of various computers using standard linear equations software in a Fortran environment," *Technical Memorandum,* No. 23, Argonne National Laboratory, Argonne, Illinois 60439, 1988.

S.-E. Sandström was born at Umea, Sweden, on September 24, 1956. He received an M.Sc. in electrical engineering and a Ph.D. in theoretical physics from Chalmers University of Technology in 1982 and 1988, respectively. His research interests include doubly periodic waveguides, channeling radiation and coherent bremsstrahlung, antenna and grating problems.

G. Tayeb was born in Marseille, France, on November 11, 1959. He graduated from the Ecole Normale Supérieure de l'Enseignement Technique and passed the Agrégation in 1981. He is currently , Maître de Conférences at the Faculté des Sciences de Saint Jérôme and a member of the Laboratoire d'Optique Electromagnetique. His thesis, hold in 1990, concerned grating problems, with a special attention to anisotropic structures.

R. Petit was born in France, on September 27, 1931. He graduated from the Ecole Normale Supérieure de Saint-Cloud, France, and passed the Agrégation in 1956. He is currently a Professor at the Faculté des Sciences de Saint-Jérôme, in Marseille, where, at the end of the sixties he founded the Laboratoire d'Optique Electromagnétique. He received a prize from the French Academy of Sciences in 1981 for his work on grating

theory. For the same reason he was nominated fellow of the OSA. He is the Editor and a coauthor of the book, *Electromagnetic Theory of Gratings,* in Current Physics Series No. 22, 1980, Springer-Verlag.